J. Synchrotron Rad. (1998). **5**, 409–411

Development of an in-vacuum minipole undulator

Toshiya Tanabe,[a]* Xavier-Marie Maréchal,[a] Takashi Tanaka,[a] Hideo Kitamura[a] and Peter M. Stefan[b]

[a]JAERI-RIKEN SPring-8 Project Team, Kamigori, Ako-gun, Hyogo 678-12, Japan, and [b]National Synchrotron Light Source, Brookhaven National Laboratory, Upton, NY 11973, USA. E-mail: ttanabe@postman.riken.go.jp

(*Received 4 August 1997; accepted 6 November 1997*)

An in-vacuum minipole (short-period) insertion device has been developed in a collaboration between SPring-8 and the National Synchrotron Light Source (NSLS). The magnetic arrays were constructed by SPring-8 and were installed in a chamber with mechanical parts in the X-ray ring (E = 2.584 GeV) at the NSLS in May 1997. The device is made of permanent magnets with 30.5 periods and a period length of 11 mm. It is designed to produce fundamental radiation at 4.6 keV, and, with a modest value of deflection parameter (K = 0.7 at 3.3 mm gap), enables higher harmonics to be used for a variety of experiments.

Keywords: insertion devices; magnets.

1. Introduction

As a convention, a 'minipole' undulator refers to an insertion device (ID) with a period length of the order of 1 cm or less. With the advent of the third-generation light source, the vertical emittance of the electron beam (e-beam) has become small enough to accommodate sub-centimeter magnet gaps without sacrificing e-beam lifetime in the storage ring. In-vacuum insertion devices allow the magnetic gap to be closed to the beam dynamics limit. With a value of K not much smaller than unity, the use of higher harmonics and modest tunability are also possible.

In §2 we describe the aim of this collaboration. Design details of the magnet blocks and holder structure are described in §3. Permeance of the magnetic circuit is one subject which calls for particular attention. §4 is devoted to magnetic field measurement and field correction of the device. Vacuum testing of the array is explained in §5 and a brief description of mechanical components is given in §6. The concern of ring impedance in the transition areas is discussed in §7.

2. NSLS-IVUN project

As a part of research activity into future SPring-8 devices, we have collaborated in the development of a device called NSLS-IVUN (in-vacuum undulator), which was installed in the X-ray ring (E = 2.584 GeV) at the NSLS in Brookhaven National Laboratory (BNL) in May 1997. The magnetic arrays are provided by SPring-8 and are installed in a vacuum chamber with mechanical and control systems developed at the NSLS.

The NSLS X-ray ring parameters as of May 1997 are given in Table 1. Despite the fact that this ring is a second-generation light source, extremely low beam coupling (~0.1%) enables us to achieve a minimum gap of 2.5 mm. Predicted radiation spectra with zero emittance and zero beam-energy spread, and one with actual finite values, are shown in Fig. 1.

Table 1
Pertinent NSLS X-ray ring parameters for IVUN operation.

	Operations lattice	Low-emittance lattice (in future)
Energy	2.584 GeV	2.584 GeV
Maximum current	430 mA	?
β_x/β_y	1.70 m/0.37 m	1.17 m/0.30 m
$\eta_x/\eta_{x'}$	−0.088/0.04	0.17/0
α_x/α_y	0.23/−0.02	−0.002/0
σ_E/σ_L (FWHM)	0.085%/13 cm	0.085%/13 cm
$\varepsilon_x/\varepsilon_y$	94 nm rad/0.1 nm rad	45 nm rad/0.1 nm rad
σ_x/σ_y	407 μm/6.2 μm	271 μm/5.6 μm
$\sigma_{x'}/\sigma_{y'}$	244 μrad/16.7 μrad	196 μrad/18.6 μrad

3. Magnet array design

An in-vacuum minipole undulator imposes extra constraints and challenges compared with conventional IDs in the design of the magnet arrays, primarily because of the following reasons: (i) a higher machining accuracy is required; (ii) the size of the good field region (horizontal field roll-off is less than 0.5%) is to be maintained while keeping reasonably high permeance values in the magnetic circuit to avoid excessive demagnetization.

As the period length decreases, the relative errors increase with a given machining accuracy. Variation in the thickness of the titanium nitride (TiN) coating, which reduces outgassing from the magnetic materials, also contributes to block size error. A construction scheme with individual independent magnet holders and clamps is not appropriate, as relative errors in machining with respect to the block size become larger and the large number of gaps created in such a structure may result in poor vacuum performance. Hence, we have developed a novel structure to place and hold small magnet pieces in precise locations; it is depicted in Fig. 2. Newly developed neodymium–iron–boron magnets with a very high intrinsic coercivity (NEOMAX 32-EH) were used. The accuracy of the side-plate period is within ±10 μm, fabricated by computer-aided machining. The thickness variation of the 5 μm-thick TiN coating is less than 1 μm. The magnet block clamps are made of BeCu to obtain a spring-like feature which ensures that force is equally exerted on all four blocks beneath.

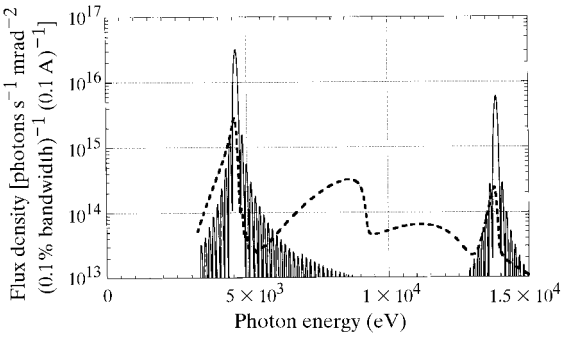

Figure 1
Calculated spectra of IVUN. The solid line is the flux density from an electron beam without emittance and energy spread. The broken line represents predicted values including those effects.

Table 2
Integrated multipole goals for NSLS X-ray ring and measured results for IVUN at SPring-8.

	Measured results	Goal
Normal/skew dipole	77/−70 G cm	100 G cm
Normal/skew quadrupole	25 G/−192 G	10 G/100 G
Normal/skew sextupole	161/41 G cm^{-1}	50 G cm^{-1}
Normal second integral	0.031 G m^{-2}	8 G m^{-2}
Skew second integral	–	8 G m^{-2}
RMS phase shake	1.45°	2°

A 100 μm Ni foil covers the magnet surface to reduce the resistive impedance of the device. Peak magnetic field reduction with the foil is only 20–30 G out of 7000 G , at a 3.3 mm gap, and no excessive field distortion was observed. Ni was chosen because of its relatively high electrical conductivity, UHV compatibility, and as its ferromagnetic nature secures the foil to the magnet surface. At the NSLS X-ray ring, a good field region of at least ±5 mm is required.

Permeance is the ratio of the magnetic flux density of the magnet to the demagnetization field (see, for example, Parker, 1990). The higher the value of permeance, the less prone the magnet is to demagnetize. A number of computer simulations indicate that horizontally magnetized blocks have lower values of permeance, on average, and thus it is the limiting factor to reduce the magnet size, and that permeance is lower with a larger gap. Therefore, a smaller gap should be preferably maintained during bake-out in order to minimize demagnetization.

4. Magnetic field measurement and field correction

4.1. *Magnetic field measurement*

Two types of magnetic field measurement system were used (see, for example, Walker, 1994): (i) a Hall-probe field mapping system and (ii) a rotating-coil field integral measurement system. We use AREPOC HHP-MP Hall probes, which have an active area of 100 × 100 μm, and the thickness of the probe enclosure is 1 mm. It is placed in a 1.5 mm-thick copper plate with duralumin support arm and sandwiched with Kapton tapes. Calibration was performed in-house using a nuclear magnetic resonance (NMR) probe (Metrolab PT2025) and a standard dipole electromagnet. Even though there is no temperature-controlling device in the enclosure of the probe, the low ($3.0 \times 10^{-4}\,K^{-1}$) temperature coefficient of the probe, software compensation and reasonable ambient temperature control ensure accuracy in the measurements. The center of the probe has been found to stay on-axis within a range of ±1 μm vertically and ±7 μm horizontally through the travel. For the longitudinal direction, the maximum deviation from the ideal position was measured using a laser interferometer and found to be within 15 μm after 500 mm travel. We have developed a continuously rotating coil system for the field integral measurement. A detailed description of this device is given elsewhere in these proceedings (Stefan *et al.*, 1998).

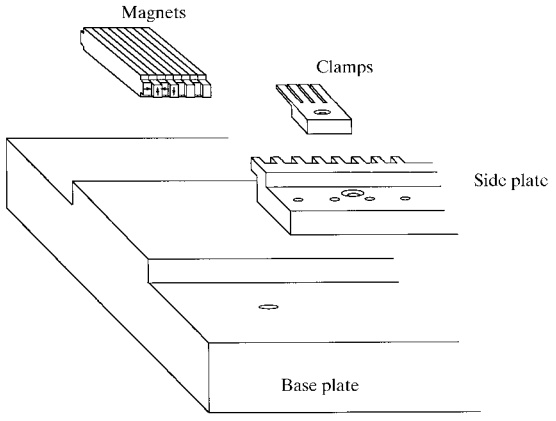

Figure 2
IVUN array structure.

4.2. *Field correction*

Field correction was made by first using simulated annealing (Cox & Youngman, 1986) for coarse correction, then inserting magnet chips on the backs of the magnets for fine adjustment. The multipole components were measured within a range of x = ±4 mm. Integrated multipole requirements for the NSLS X-ray ring and our measurement results are presented in Table 2. The field correction was made by chip magnets. Fig. 3 shows the gap-dependence of the final values of integrated dipoles and quadrupoles.

5. Ultra-high-vacuum (UHV) testing

After the magnetic field correction was finished, a vacuum test in a UHV chamber was conducted to make sure that no objectionable elements outgas from the magnet arrays. The temperature of the magnets was maintained to not exceed 398 K. Three types of vacuum gauges were used: a cold cathode gauge (CCG) for low vacuum, a nude Bayard Alpert gauge (BAG) and an extractor gauge (EXG) for UHV. Fig. 4 shows the vacuum

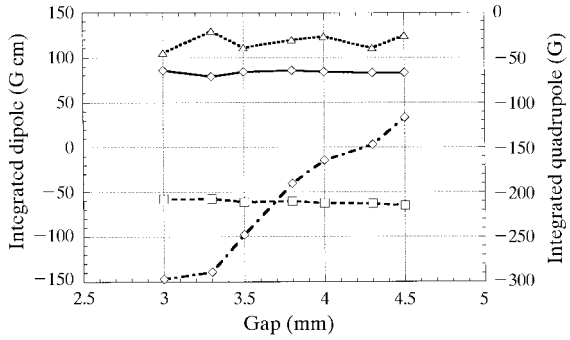

Figure 3
Gap dependence of integrated multipole components: normal dipole (solid line), skew dipole (dashed line), normal quadrupole (dotted line) and skew quadrupole (dash-dotted line).

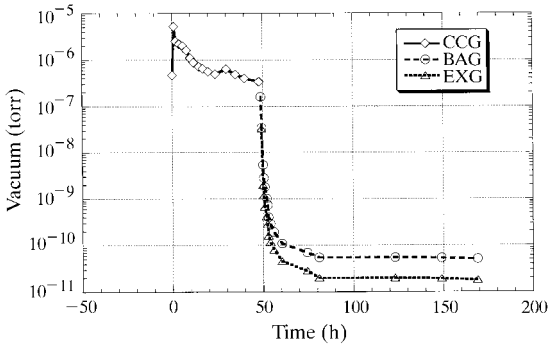

Figure 4
Elapsed time *versus* the vacuum gauge reading in the UHV test.

readings from the various gauges *versus* elapsed time. The difference between the reading of the BAG and the EXG in the final hours comes from the fact that the BAG has approached its X-ray limit while the EXG limit is still lower. The final value of the vacuum read by the EXG (IONIVAC IM520, Leybold) was 2×10^{-9} Pa, which implies adequate UHV compatibility of the arrays.

6. Mechanical support and vacuum system (BNL)

IVUN is composed of three major components: a rectangular vacuum chamber with bellows feedthroughs, magnet array units with drive system, and an elevator base stage, upon which all of the above components are supported. The chamber is equipped with three forms of pumping: a $300\,l\,s^{-1}$ ion pump, a titanium sublimator and a non-evaporable getter. The undulator magnet arrays are mounted on the water-cooled beams of the drive system, directly in the accelerator ultra-high vacuum. The drive system enables magnet gaps between 2 mm and 10 mm. The elevator base stage provides mounting fixtures for the IVUN vacuum chamber and the undulator magnet drive. In addition, it provides a ± 3 mm vertical translation of the combined chamber/magnet assembly about the nominal beam height.

7. Transition area

According to Bane & Krinsky (1993, 1994), there are three predominant beam dynamic effects caused by the small-gap aperture of a minipole undulator and by the aperture change due to the transition from the outer vacuum chamber to the ID: (i) power dissipation due to longitudinal-impedance transverse-coupled-bunch instability, (ii) strong head–tail instability caused by transverse resistive impedance, and (iii) transverse geometric impedance. For a stainless steel surface with a 2 mm gap and single-bunch e-beam current of 0.1 A, the power dissipation is found to be only 19 W. The only concern here is the possibility that the continuity sheet is detached from the magnet array so that heat has essentially no place to escape. For this reason we have decided to use a 100 μm Ni sheet, even though it is ferromagnetic. It can be shown that at the gap being smaller than 4 mm, the transverse resistive impedance becomes dominant, as it is inversely proportional to the third power of the gap value, whereas the geometric impedance only varies as the first power.

8. Conclusions

With an in-vacuum structure, a minipole undulator having modest tunability and useful harmonics has been constructed. The magnetic field quality is found be satisfactory, after spectral and multipole correction, and the magnet arrays show excellent UHV compatibility. The completed device was installed in the X13 R&D straight section of the NSLS X-ray ring in May 1997 and successful commissioning of the device was carried out in June 1997.

References

Bane, K. & Krinsky, S. (1993). BNL Informal Report BNL-48792. BNL, Upton, NY 11973, USA.
Bane, K. & Krinsky, S. (1994). *Proc. 1993 PAC*, pp. 3375–3377.
Cox, A. & Youngman, B. (1986). *Proc. SPIE*, **582**, 91–97.
Parker, R. J. (1990). In *Advances in Permanent Magnetism.* New York: Wiley-Interscience.
Stefan, P. M., Tanabe, T., Krinsky, S., Rakowsky, G., Soloman, L. & Kitamura, H. (1998). *J. Synchrotron Rad.* **5**, 417–419.
Walker, R. P. (1994). In *Synchrotron Radiation Sources: Magnetic Measurement.* Singapore: World Scientific.